

Novel GMR Sensor for Estimation of Magnetic Nanoparticles inside Minute Cavities

メタデータ	言語: eng 出版者: 公開日: 2017-11-16 キーワード (Ja): キーワード (En): 作成者: 山田, 外史, 岩原, 正吉, 柿川, 真紀子, C.P., Gooneratne, Sotoshi, Yamada, Masayoshi, Iwahara, Makiko, Kakikawa, Y., Matsumoto メールアドレス: 所属:
URL	https://doi.org/10.24517/00048916

This work is licensed under a Creative Commons Attribution 3.0 International License.



Novel GMR Sensor for Estimation of Magnetic Nanoparticles inside Minute Cavities

C. P. Gooneratne, S. Yamada, M. Iwahara, M. Kakikawa and Y. Matsumoto
Institute of Nature and Environmental Technology, Kanazawa University

Utilization of magnetic nanoparticles in biomedicine has seen an unprecedented growth in recent years. The ability to accurately estimate magnetic nanoparticles inside small areas of the body provides an advantage in hyperthermia therapy, a form of cancer treatment. This paper concentrates on a novel giant magnetoresistance (GMR) needle-type sensor to detect and estimate low concentration magnetic fluid inside minute agar cavities injected with magnetic fluid. Theoretical analysis, experimental results and information on the fabricated GMR needle-type sensor are reported. The experimental results show a favorable agreement to the analytical analysis, supporting the potential use of the GMR needle-type sensor in hyperthermia therapy.

Key Words: giant magnetoresistance, hyperthermia therapy, magnetic nanoparticles, demagnetizing factor

1. Introduction

Hyperthermia therapy exploits the self heating capability and the biocompatibility of magnetic nanoparticles, as well as the sensitivity of tumor cells to temperatures in excess of 41°C [1]. Magnetic fluid consists of superparamagnetic particles of Fe_3O_4 and other magnetic particles, modified or coated with different types of biopolymer or synthetic polymer [2]. In hyperthermia therapy magnetic fluid injected into the tumor cell and an alternating magnetic field is applied [3]. Heat is produced due to the hysteresis loss of the magnetic nanoparticles. Prolonged exposure of the tumor cells to elevated temperatures destroys the tumor.

Ideally hyperthermia therapy is performed on non-invasive, *in situ* tumors which are normally detected when they are small and confined [3]. In these cases (tumor diameter less than 20 mm) the cancer has not spread to other organs. Low concentration magnetic fluid (less than 2.8 % weight density, D_w (mgFe/ml)) is generally used in hyperthermia therapy, to keep the dose in the body as low as possible. However, once injected the magnetic fluid tends to spreads inside tissue, further decreasing the low concentration weight density. The specific heat capacity required to destroy a tumor is proportional to ac magnetic field amplitude, frequency and weight density as well as quality of treatment [4]. Hence, it is vital that the magnetic fluid weight density be known inside the body before as well as after treatment (to check for

remnant density). This paper proposes a novel giant magnetoresistance (GMR) needle-type sensor that can be inserted into the body in a low-invasive way to detect and estimate low-concentration magnetic fluid weight density in initial stage *in situ* tumors for successful implementation of hyperthermia therapy.

2. Theoretical Analysis

2.1 Relationship between magnetic fluid weight density and relative permeability

Figure 1 (a) shows magnetic fluid used for clinical applications. It is assumed that the magnetic nanoparticles are uniformly distributed in the fluid. They are also assumed to be cylindrical in shape where the height is equal to the diameter. Also, assuming that the relative permeability of magnetic nanoparticles are infinity and that of liquid is one, the permeance of an equivalent magnetic path through magnetic nanoparticles and air is estimated. Thus, the equivalent permeance of a unit volume is obtained and the relative permeability is derived [4]. However, it can be seen from Fig. 1 (b) that the magnetic nanoparticles in the magnetic fluid have a cluster structure. Hence, it is assumed that it is also uniformly distributed as shown in the spherical structure of the model (Fig. 1 (c)). The space factor of spherical magnetite is also obtained due to space between the nanoparticles. The equation relating the permeability to magnetic fluid weight density can then be written as,

$$\mu' = 1 + C_d D_w / h_s \gamma_f \quad (D_w \ll 1) \quad (1)$$

where C_d is a coefficient (theoretically 4), $\gamma_f = 4.58$ is the specific gravity of magnetic bead (W-35

Correspondence: C. P. Gooneratne, Institute of Nature and Environmental Technology, Kanazawa University, Kanazawa 920-1192, Japan
email: chinthaka.gooneratne@gmail.com

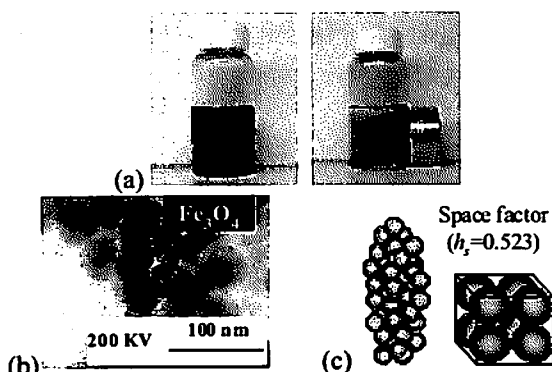


Fig. 1 Magnetic fluid characteristics. (a) Magnetic fluid. (b) Electron microscopy image. (c) Spherical type model of magnetite.

sample – Taiho company) and $h_s = 0.523$ is the space factor of spherical magnetite.

Equation (1) shows that the relative permeability is proportional to the weight density but independent of shape or size. Experiments were performed by a vibrating sample magnetometer (VSM) where the relative permeabilities of various magnetic fluid weight densities were obtained. Figure 2 shows the comparison of the analytical results to experimental results. The relative permeability is proportional to the magnetic fluid weight density.

2.2 Magnetic fluid weight density estimation

The shape of tumors can be estimated to be spherical in shape. If an uniform magnetic flux density (B_0) is applied to such a tumor that is injected with magnetic fluid as shown in Fig. 3, flux lines will converge at the tumor. The magnetic flux density at the center of the tumor (B_1) can be expressed as follows.

$$B_1 = \mu^* B_0 / \left\{ 1 + N(\mu^* - 1) \right\} \quad (\mu^* \approx 1) \quad (2)$$

where N is the demagnetizing factor of the cavity [4]. The difference between the applied magnetic flux

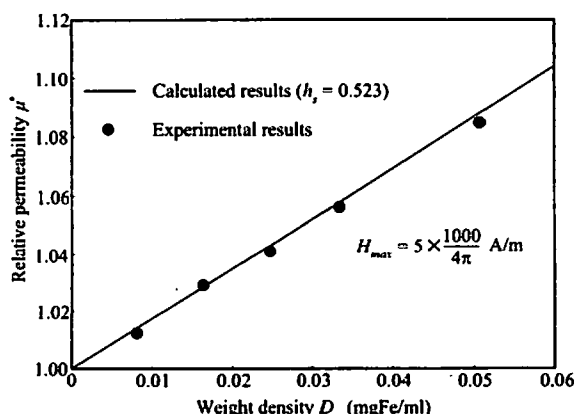


Fig. 2 Relationship between relative permeability and magnetic fluid weight density.

density and the magnetic flux density inside the tumor can be obtained by substituting Eq. (1) into Eq. (2) and expressed as,

$$\delta = (B_1 - B_0) / B_0 \times 100 \approx C_d (1 - N) D_w / (h_s \gamma_f) \times 100 \% \quad (D_w \ll 1) \quad (3)$$

Equation (3) shows that while the weight density can be calculated from the applied magnetic flux and the magnetic flux at the center of the tumor, the shape of the tumor has an influence due to the presence of N .

2.3 Error analysis due to variation of shape of tumor

Given that a cavity is spherical or ellipsoidal, magnetic nanoparticles can be assumed to uniformly distribute inside. However, the exact shape and the size of the area are difficult to predict when magnetic fluid is injected into the tumor during hyperthermia therapy. Hence, the accuracy of the estimated value with regards to the shape of the cavity should be considered.

Consider the errors of N and D_v as follows:

$$D_v = \langle D_v \rangle + \Delta D_v \quad (4)$$

$$N = \langle N \rangle + \Delta N \quad (5)$$

where $D_v = D_w / h_s \gamma_f$ is the magnetic fluid volume density, $\langle D_v \rangle$ and $\langle N \rangle$ are the expected mean values, and ΔD_v and ΔN are errors. Equations (4) and (5) are substituted into Eq. (3) to obtain Eqs. (6) and (7).

$$\delta = C_d (1 - \langle N \rangle - \Delta N) (\langle D_v \rangle + \Delta D_v) \quad (6)$$

And

$$\frac{\Delta D_v}{\Delta N} = \frac{\langle D_v \rangle}{1 - \langle N \rangle} \quad (7)$$

Then finally the following equation is obtained.

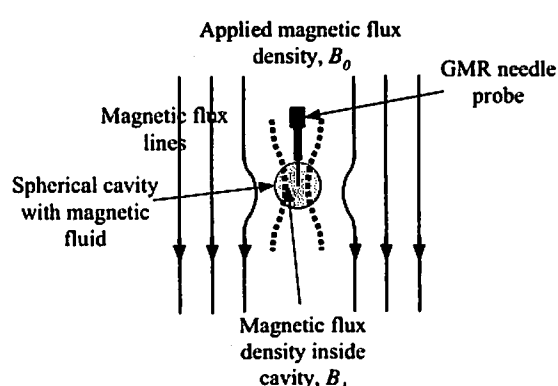


Fig. 3 Magnetic flux distribution in a magnetic fluid filled spherical cavity.

$$\frac{(\Delta D_v / \langle D_v \rangle)}{(\Delta N / \langle N \rangle)} = \frac{I}{(1/\langle N \rangle) - I} \quad (8)$$

It is assumed that if the tumor has a spherical structure ($N = 1/3$) the injected area can vary between $N = 0.25$ (long ellipsoidal, aspect ratio $s = (\text{long axis } b)/(\text{diameter } a) \approx 1.4$) and $N = 0.5$ (flat ellipsoidal, $s \approx 0.6$). Then the shape of the mean value $\langle N \rangle = 0.375$ and $s \approx 0.864$. Then Eq. (8) is written as,

$$\frac{\Delta D_v}{\langle D_v \rangle} = 0.6 \frac{\Delta N}{\langle N \rangle} \quad (9)$$

And if $(\Delta N / \langle N \rangle)$ is 1/3 we obtain,

$$\frac{\Delta D_v}{\langle D_v \rangle} = 0.2 \quad (10)$$

Equation (10) shows that the maximum error is 20 %. Experiments are performed in this paper by inserting the sensor needle in magnetic fluid filled cylindrical agar cavities. The magnetic flux density is not uniform inside the agar cavities so the position of the sensor needle is important. It is assumed that there could be some positioning error within a spherical area of 2.5 mm radius. Figure 4 shows the results obtained by numerical analysis for the condition of the cavity to be within the 20 % error limit (N anywhere within the spherical area between 0.25 and 0.5).

3. Experimental Apparatus

3.1 GMR needle-type sensor

A novel GMR sensor was fabricated with a needle as shown in Fig. 5. The needle tip has a GMR sensing area of $75 \mu\text{m} \times 40 \mu\text{m}$ which can be inserted into the body in a low-invasive way. The GMR sensors are arranged as a bridge circuit and the three other sensors that make up the bridge is located near the bonding pads. This gives rise to the possibility of measuring magnetic flux density inside the tumors and the applied magnetic flux density, simultaneously. These features are advantageous in a clinical environment. The sensitivity of the sensor is approximately $12.5 \mu\text{V}/\mu\text{T}$ in the sensing direction.

3.2 Experimental setup

The experimental setup as shown in Fig. 6 consists of the GMR needle-type sensor tip setup in the center of a Helmholtz tri-coil. The Helmholtz tri-coil is a variant of [5] and provides a uniform

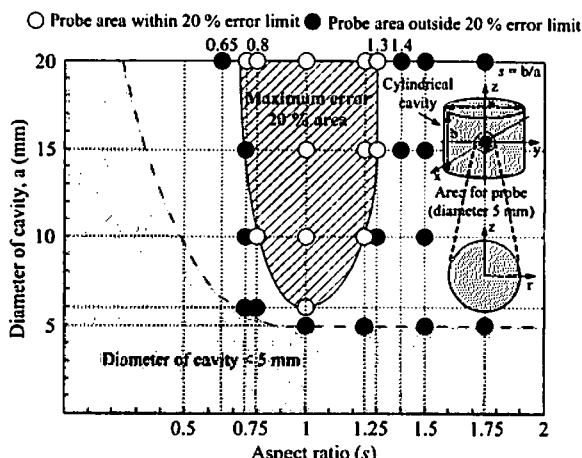


Fig. 4 Relationship between diameter of cavity, aspect ratio and error.

magnetic flux density (fluctuation $\leq 0.01\% - 0.03\%$ m in the axial and radial direction, from the midpoint). The agar/potato starch model used for experiments is placed on a tray and moved up, so the needle tip is at the center of the magnetic fluid filled agar cavity. Experiments are performed with $100 \mu\text{T}$ magnetic flux density at 100 Hz.

4. Experimental Results

4.1 Detection of magnetic fluid

Experiments were performed by injecting low-concentration magnetic fluid (0.814 % D_w) into cylindrical agar pieces ($s = 1$, $N = 0.33$) as shown in Fig. 6. The diameters of the agar pieces were chosen to be between 4 – 14 mm to simulate in situ tumors, which are generally less than 20 mm. Fig. 7 shows that when the needle tip of the sensor is inserted at 10 mm intervals, the GMR sensor can detect the magnetic nanoparticles injected into agar pieces with diameter as low as 4 mm. The change in signal corresponds to the difference between the signal obtained for the magnetic fluid filled agar and potato starch (reference medium). The signal does not

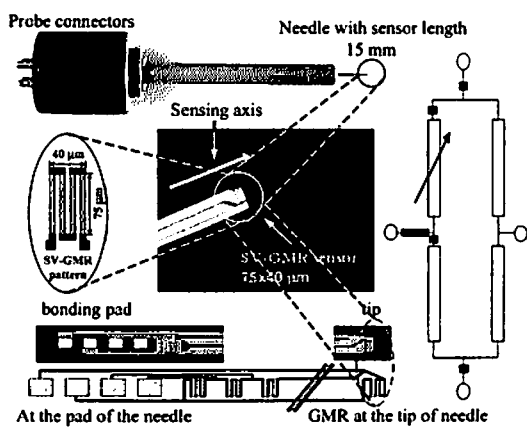


Fig. 5 GMR needle-type sensor.

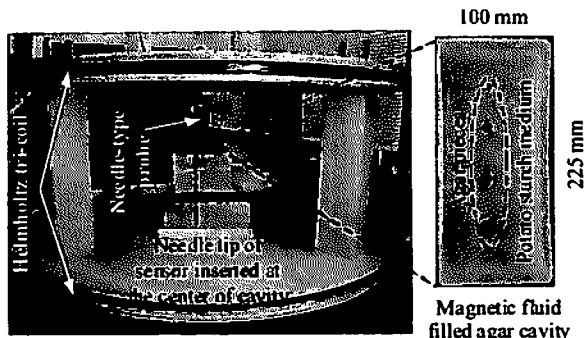


Fig. 6 Experimental setup.

differ too much between the four samples which indicate that if N stays the same the change in magnetic flux density will only be influenced by D_w , therefore verifying Eq. (3).

4.2 Estimation of magnetic fluid

Agar pieces of diameter and height 18 mm ($s = 1$) were injected with low-concentration magnetic fluid and the GMR needle-type sensor was inserted to the middle of the cavity. Fig. 8 shows that the magnetic fluid weight density is proportional to the change in magnetic flux density. The theoretical lines for $s = \infty$, 1 and 0.5 are based on ellipsoidal cavities. Magnetic fluid weight densities as low as 0.145 % was estimated by the GMR needle-type sensor.

5. Conclusion

This paper proposes a novel GMR needle-type sensor that can be inserted inside the body in a low-invasive way. Experiments were performed by injecting low weight density magnetic fluid into cylindrical agar pieces simulating stage 1 tumors. The GMR needle-type sensor was able to detect and estimate the magnetic fluid inside the agar pieces. Since the shape and size of the cavity influences measurement further analysis should and will be performed to incorporate tumors of various sizes. A

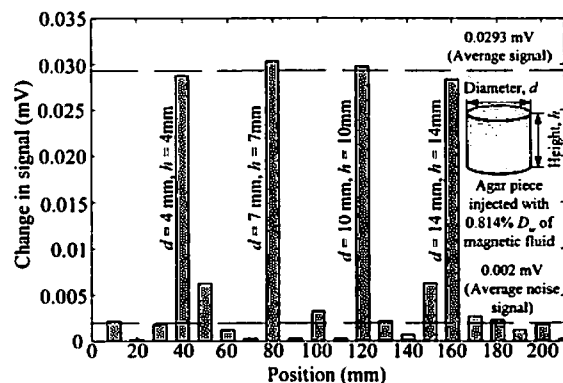


Fig. 7 Detection of magnetic fluid.

comprehensive error analysis was presented with regards to the aspect ratio and the diameter of cavity.

References

- [1] C. C. Berry and A. S. G. Curtis, "Functionalisation of magnetic nanoparticles for applications in biomedicine", *J. Phys. D: Appl. Phys.* Vol. 36, pp. R198-R206, 2006.
- [2] D. Bahadur and J. Giri, "Biomaterials and magnetism", *Sadhana*, Vol. 28, Parts 3 and 4, pp. 639-656, 2003.
- [3] I. Hilger, R. Hergt and W. A. Kaiser, "Towards breast cancer treatment by magnetic heating", *Journal of Magnetism and Magnetic Materials*, Vol. 293, pp. 314-319, 2005.
- [4] S. Yamada, K. Chomsuwan, S.C. Mukhopadhyay, M. Iwahara, M. Kakikawa and I. Nagano, "Detection of Magnetic Fluid Volume Density with a GMR Sensor", *J. Magn. Soc. Jpn*, Vol. 31, pp. 44-47, 2007.
- [5] I. Sasada, Y. Nakashima, "A planar coil system consisting of three coil pairs for producing uniform magnetic field". *J. Appl. Phy*, Vol. 99(8), pp. 08D904-08D904-3, 2006.

Received: 27 November 2008/Revised: 17 March 2009

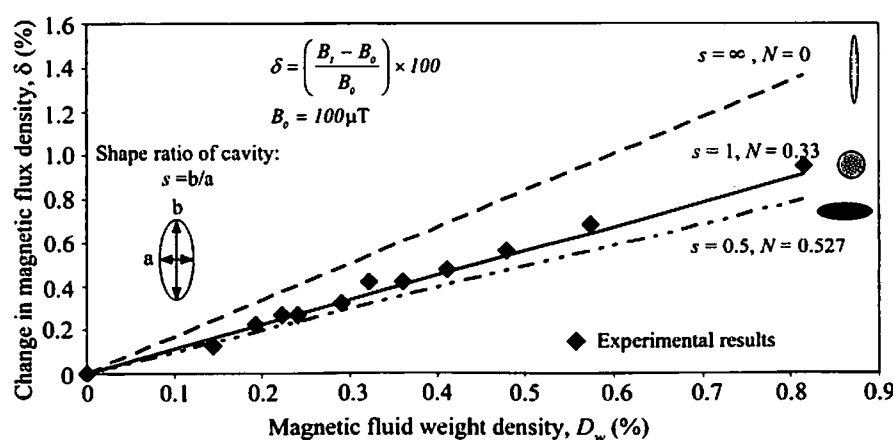


Fig. 8 Estimation of low-concentration magnetic fluid weight density.